Developmental Biology 454 (2019) 118–127

Contents lists available at ScienceDirect

Developmental Biology

journal homepage: www.elsevier.com/locate/developmentalbiology

Proteomics and single-cell RNA analysis of *Akap4*-knockout mice model confirm indispensable role of *Akap4* in spermatogenesis

Xiang Fang [a,1], Ling-Long Huang [a,d,1], Jian Xu [b], Cai-Qi Ma [b], Zhi-Heng Chen [b], Zhan Zhang [a], Cai-Hua Liao [a], Shu-Xin Zheng [a], Peng Huang [c,d], Wen-Ming Xu [e], Na Li [a,*], Ling Sun [b,**]

[a] Guangzhou Institute of Pediatrics, Guangzhou Women and Children's Medical Center, Guangzhou Medical University, Guangzhou, China
[b] Center of Reproductive Medicine, Guangzhou Women and Children's Medical Center, Guangzhou Medical University, Guangzhou, China
[c] Department of Urology, Okayama University Graduate School of Medicine, Dentistry and Pharmaceutical Sciences, Okayama, Japan
[d] Department of Urology, Zhujiang Hospital, Southern Medical University, Guangzhou, China
[e] Reproductive Endocrinology and Regulation Laboratory, Key Laboratory of Obstetric, Gynecologic and Pediatric Diseases and Birth Defects of Ministry of Education, West China Second University Hospital, Sichuan University, Chengdu, China

ARTICLE INFO

Keywords:
Akap4
Spermatogenesis
Fibrous sheath
Haspin
Ccdc38

ABSTRACT

Sperm fibrous sheath, a unique cytoskeletal structure, is implicated in various sperm physiological functions, such as sperm maturation, motility and capacitation. *AKAP4* has been described to be required for structural and functional integrity of the fibrous sheath. We generated *Akap4*-knockout mice line using CRISPR-Cas9 system. Cytomorphology and motility of sperm and testes were studied, confirming loss of Akap4 led to abnormal sperm morphology, motility and infertility. The proteomic components of testes were studied and Akap4 was found to be significantly decreased in the *Akap4*-knockout mice. Testis single-cell RNA sequencing and analysis revealed three genes with significant change in the general cell population, i.e., *Akap4*, *Haspin*, and *Ccdc38*. The single-cell RNA expression profiles also showed that the major difference between *Akap4*-knockout and wild-type testes existed in the elongating cell cluster, where in the *Akap4*-knockout testes, a subgroup of elongating cells with marker genes involved in cell adhesion and migration were increased, while a subgroup of elongating cells marked by mitochondrial sheath genes were decreased. Our results revealed the complex and well-coordinated procedures of spermatogenesis, and substantiated *Akap4*'s indispensable roles in the integrity of sperm flagellum and the stepwise maturation of spermatozoa.

1. Introduction

Male-attributable infertility accounts for about 20%–50% of cases of infertility (Hamada et al., 2012). The presence of a male factor is often diagnosed by the finding of abnormal sperm parameters (i.e. morphology and motility). The sperm tail controls sperm motility and aids in penetration of the oocyte, which is essential for fertilization (Miki et al., 2002). Sperm flagellum is structurally divided into three observable parts: the middle piece, the principal piece, and the end piece, all with the axoneme as the core (Fawcett, 1975). The principal piece occupies approximately three quarters of the length of the flagellum and acts as the main structure driving sperm motility (Turner, 2003). In the middle piece, the mitochondrial sheath and the outer dense fibers are surrounding the core. In the principal piece, the mitochondrial sheath and part of outer dense fibers are replaced by fibrous sheath. The fibrous sheath is a unique cytoskeletal structure, which provides the sperm tail with mechanical support that modulates flagellar bending and defines the shape of the flagellar beat (Fawcett, 1975). Furthermore, the fibrous sheath is assumed to serve as a scaffold for proteins in signaling pathways involved in sperm maturation, motility, capacitation, and glycolysis (Eddy et al., 2003).

Akap4 (A kinase anchor protein 4; also called fibrous sheath

* Corresponding author.
** Corresponding author.
E-mail addresses: fangx@cougarlab.org (X. Fang), huangll@cougarlab.org (L.-L. Huang), 284374434@qq.com (J. Xu), phelix-ma@foxmail.com (C.-Q. Ma), chzhh2003@126.com (Z.-H. Chen), zhangz@cougarlab.org (Z. Zhang), liaoch@cougarlab.org (C.-H. Liao), zsx@cougarlab.org (S.-X. Zheng), huangpeng509@gmail.com (P. Huang), Xuwenming@scu.edu.cn (W.-M. Xu), lina@cougarlab.org (N. Li), sunling6299@163.com (L. Sun).
[1] Equal contribution.

https://doi.org/10.1016/j.ydbio.2019.06.017
Received 22 February 2019; Received in revised form 15 May 2019; Accepted 20 June 2019
Available online 28 June 2019

component 1 or AKAP 82) is the first AKAP to be described as associated with the sperm flagellum (Carrera et al., 1994) and is the most abundant protein in the sperm fibrous sheath (Miki et al., 2002; Eddy et al., 2003). AKAPs are a conserved family composed of around 50 scaffold proteins which compartmentalize protein phosphorylation by tethering cyclic AMP (cAMP)-dependent protein kinase (PKA) regulatory subunits to various cellular structures (Kumar et al., 2017). Targeted disruption of the *Akap4* gene by CRE/loxP method was reported in mice (Miki et al., 2002). *Akap4*-knockout (KO) mice produce normal numbers of spermatozoa but sperm fail to show progressive motility and male mice are infertile. These sperm have shortened flagella and have reduced or absent proteins that are normally associated with the fibrous sheath, such as Akap3, RII alpha, Gapds. The axonemal and outer dense fibers are intact, although the fibrous sheath is incomplete, resulting in a thinner principal piece and a shorter flagellum with an amorphous structure. In humans, defective *AKAP4* was reported to be related with asthenozoospermia and may explain a part of infertile cases with multiple morphological abnormalities of the sperm flagella (MMAF) (Baccetti et al., 2005). Besides, *Cabyr*-knockout male mice also showed a defect in sperm motility, a significant disorganization in the fibrous Sheath, as well as abnormal configuration of doublet microtubules, suggesting that the fibrous sheath is important for the correct organization of the axoneme (Young et al., 2016). Recent study found that deletion of a novel MMAF candidate gene, *Q*rich2 in mice, lead to decreased expression of *Akap4*, indicating that *AKAP4* as a central player in regulating of sperm flagella development and motility (Shen et al., 2019). The biological functions of the fibrous sheath and its associated proteins have not been fully understood. Using the CRISPR/Cas9 genome editing system, researchers are able to produce genetically modified mice to study male infertility more rapidly, efficiently, and inexpensively (Shen et al., 2019). To investigate the structure and function of fibrous sheath, we utilized the CRISPR-Cas9 system to generate an *Akap4*-knockout mouse line. Single RNA sequencing and proteomic analysis were used to decipher the function of genes in higher resolution. Therefore, using these tools, our goal is to recapitulate the molecular scenario of defective *Akap4* and its influence on the development of male gametes.

2. Materials and methods

2.1. Generating Akap4-KO mice

Akap4-KO mouse line was generated by non-homologous end joining (NHEJ) using CRISPR/Cas9 method in Shanghai Biomodel Organism Science and Technology Development Co., Ltd. All mice used in this study were maintained on a C57BL/6J genetic background. The *Akap4* gene (ENSMUSG00000050089) is located on the X-chromosome and includes 6 exons. Production of Cas9 mRNA and small guide RNAs (sgRNA) was performed as previously described (Shen et al., 2013). Four sgRNAs were designed, targeting the fourth exon of *Akap4* gene. Superovulated female C57BL/6J mice (6–8 weeks old) were mated with males, and the fertilized embryos were collected from the oviducts. The mixture of Cas9 mRNA and sgRNA were injected into the fertilized eggs with recognized pronuclei in M2 medium. The injected zygotes were cultured at 37 °C with 5% CO_2 in air, and the obtained blastocysts were then transferred into the uterus of pseudopregnant C57BL/6J females. PCR was carried out to genotype the newborns. The genotyping primers were as follows: forward: 5' CCAGATCAGTGATCCTAACTAA3' and reverse: 5' GACCTCAGTACCTAGACCCTAA 3'. F1 mice were obtained and genotyped after the selected F0 mice mated with wild type C57BL6/J mice.

2.2. Evaluating structure and function of sperm and testis of wild-type and Akap4-knockout mice

Fertility was tested in the male mice of different genotypes (8–12 weeks, n = 6). Each male mouse was caged with two wild-type (WT) females (4–6 weeks). Vaginal plug was checked every morning, and once a vaginal plug was identified (day 1 post coitus), the male was allowed to rest for 2 days, after which another female was placed in the cage for another round of mating. The female was deemed as not pregnant if it did not generate any pups by day 22 post coitus, and it was euthanized to confirm the lack of pregnancy. The fertility test lasted for 3 weeks.

Cauda epididymal sperm were collected from 3- to 4-month-old male mice by incubating minced cauda epididymis in SpermRinse medium (Vitrolife, Sweden) at 37 °C for 10 min. Sperm were examined by phase microscopy. The length of spermatozoa from mutant mice was expressed relative to the length of sperm from wild type mice. Sperm viability was determined by using the Sperm Cytomorphology Analyzer with phase microscopy (Microptic S.L., Spain). Sperm motility was observed before and after incubation in SpermRinse medium at 37 °C for 4 h in the presence or absence of 5 mM dibutyryl cAMP. Alternatively, hyperactivated motility was induced by incubating sperm in M16 medium at 37 °C for 2 h in 5% CO2 and air. Papanicolaou staining of sperm was performed following the manufacturer's instructions (Leagene Biotechnology # DA0191, Beijing, China).

Testes tissues were surgically removed, fixed in formalin and embedded in paraffin. Then 5 μm thick histologic sections were prepared. The histologic sections were stained with hematoxylin-eosin to observe the morphology with an optical microscope (Olympus, Tokyo, Japan). PAS staining was also conducted on sections from the testis using periodic acid solution and Schiff's reagents (cat. no. 395B, Sigma-Aldrich, USA).

Sperm were isolated for scanning electron microscopy as described above, washed in PBS, and fixed in 2.5% glutaraldehyde and 2% paraformaldehyde in 0.15 M sodium phosphate buffer overnight at 4 °C. Sperm were washed in the buffer and collected on Nucleopore filters or glass coverslips, subjected to critical point drying, and coated with gold/palladium. Samples were examined in a HITACHI S–3000N scanning electron microscope at 20 KV.

For transmission electron microscopy, testis and sperm from cauda epididymides were fixed under the same conditions, postfixed in 2% osmium tetroxide in cacodylate buffer, and embedded in Lowicryl resin. Sections were stained with uranyl acetate and lead citrate, and then examined in a HITACHI H-7500 transmission electron microscope at 80 kV.

2.3. Tandem mass tag (TMT) proteomic analysis of testis of wild-type and Akap4-knockout mice

The testis of WT and KO mice were milled to powder in a mortar with liquid nitrogen, and then mixed with lysis buffer in a glass homogenizer. The homogenate was incubated on ice and then centrifuged at 12000 g for 15 min at 4 °C. The supernatant protein concentration was determined with a Bradford assay. The supernatant protein was digested with Trypsin Gold (Promega, Madison, WI) at 37 °C for 16 h. After that, peptide was desalted with C18 cartridge and dried by vacuum centrifugation. Desalted peptides were labeled with TMT10-plex reagents (TMT10plex™ Isobaric Label Reagent Set, Thermofisher), and peptides were dissolved in 30 μl of 0.1 M triethylammonium bicarbonate solution (TEAB, pH 8.5), and the labeling reagent was added to 20 μl of acetonitrile. After incubation for 1 h, the reaction was stopped with 50 mM Tris/HCl (pH 7.5). TMT-labeled peptide mix was fractionated using a C18 column on a Rigol L3000 HPLC operating at 1 ml/min. Mobile phases A and B were used to develop a gradient elution. The tryptic peptides were monitored at UV 214 nm. Eluent was collected every minute and then merged to 15 fractions. The samples were dried under vacuum and reconstituted for subsequent analyses. Fractions from the first dimension RPLC were dissolved with loading buffer and then separated by a C18 column. A series of adjusted 60 min gradients according to the hydrophobicity of fractions eluted in 1D LC with a flow rate of 300 nL/min was applied. HF-X mass spectrometer was operated in positive polarity mode with capillary temperature of 320 °C. Full MS scan resolution was set to 60000 with AGC target value of 3e6 for a scan range of 350–1500 m/z.

The resulting spectra from each fraction were searched separately against databases by the search engines, i.e., Proteome Discoverer 2.2 (PD 2.2, Thermo). A maximum of 2 miscleavage sites were allowed. For protein identification, protein with at least 1 unique peptide was identified at FDR less than 1.0% on peptide and protein level, respectively. Proteins containing similar peptides and could not be distinguished based on MS/MS analysis were grouped separately as protein groups. The protein quantitation results were statistically analyzed by Mann-Whitney Test, the significant ratios, defined as $p < 0.05$, were used to screen the differentially expressed proteins (DEP). Gene Ontology (GO) and InterPro (IPR) analysis were conducted using the interproscan-5 program against the non-redundant protein database (including Pfam, PRINTS, ProDom, SMART, ProSiteProfiles, PANTHER), and the databases COG and KEGG were used to analyze the protein family and pathway. The probable interacting partners were predicted using the STRING-db server (http://string.embl.de/) based on the related species. The enrichment pipeline was used to perform the enrichment analysis of GO, IPR, COG and KEGG, respectively.

2.4. Single-cell RNA sequencing and data analysis of testis of wild-type and Akap4-knockout mice

Single-cell suspensions from isolated mouse testis were prepared by tissue mincing and enzyme digestion as previously described (La Salle et al., 2009). Briefly, the testis was excised and the tunica albuginea was removed. Seminiferous tubules were digested with Collagenase IV (Sigma Aldrich, C5138), Trypsin from bovine pancreas (Sigma Aldrich, T9201) and DNase I from bovine pancreas, lyophilized (USB, 14365), filtered, and resuspended.

We loaded ~5000 cells into 1 channel of the Chromium system for each sample and prepared libraries according to the manufacturer's protocol (10x Genomics). Sequencing reads were generated by Illumina HiSeqX10 in a paired-end 150 bp mode, and were demultiplexed by using CellRanger (3.0.0, 10X Genomics) mkfastq. The strategy for in-silicon analysis of single cell data of wildtype (WT) and *Akap4*-knockout (KO) was shown in the ensemble workflow of computational procedure (Fig. S1). Trimmomatic software was used to remove adapters, low-quality reads and low-quality bases (Bolger et al., 2014). FastQC was used to perform basic statistics on the quality of the clean data reads. The clean reads were aligned to the murine reference genome (mm10), filtered, and counted using the CellRanger count command.

The CellRanger counts for different samples were combined through CellRanger aggr. The R package Seurat (2.3.4) was applied to perform linear and nonlinear dimensional reduction (Satija et al., 2015). Only the genes expressed in more than 10 cells were reserved, and single cells with more than 200 expressed genes were retained. Quality control measures for single-cell RNA-Seq (gene count per cell, UMI count per cell, percent of mitochondrial transcripts) were also calculated. After normalization, 472 variable genes were kept for the principal component analysis (PCA). Jackstraw with 1000 replicates analysis was used to determine statistically significant principal components (PCs) to separate the cells. PCs 1–12 were selected to perform the RunTSNE function and the FindClusters function (resolution = 0.75). Twelve clusters were obtained for WT and KO, respectively. The FindAllMarkers function of Seurat was used to identify the marker genes for Cluster 1–12.

2.5. Cell type assignment

Green et al. identified 4908 marker genes for 11 major cell types in murine seminiferous tubule by single-cell RNA-Seq (Green et al., 2018). The corresponding cell types of clusters 1–12 were preliminarily recognized after comparing our marker genes with those identified by Green et al. Some clusters were recognized as the same cell types. The cluster 2 (KO_2 and WT_2), 4 (KO_4 and WT_4), 5 (KO_5 and WT_5) and 8 (KO_8 and WT_8) were recognized as Elongating spermatids; the cluster 3 (KO_3 and WT_3) and 11 (KO_11 and WT_11) were recognized as Round spermatids; the cluster 6 (KO_6 and WT_6) and 10 (KO_10 and WT_10), as well as the cluster 7 (KO_7 and WT_7) and 12 (KO_12 and WT_12), were recognized as Spermatogonia and Somatic cells, respectively. The cluster 1 (KO_1 and WT_1) and 9 (KO_9_and WT_9) were recognized as Spermatocytes and Unknown cells, respectively.

2.6. Analysis of the Elongating cells

Eight clusters of KO and WT (KO_2 and WT_2, KO_4 and WT_4, KO_5 and WT_5, as well as KO_8 and WT_8) which were recognized as Elongating spermatids were extracted and analyzed. The differential expressed genes were identified with the function FindMarkers performed on the corresponding KO and WT clusters.

2.7. Combining clusters

The RenameIdent function of Seurat was used to combine the clusters assigned to the same cell types, resulting in 12 merged clusters (6 KO and 6 WT). The markers of the merged clusters were identified with the Function FindAllMarkers and the cell types were recognized again.

2.8. Identification of total differentially expressed genes

The total differentially expressed genes between WT *and* KO were identified using the function FindMarkers (min.pct = 0.3, logfc.threshold = 0.5, min.diff.pct = 0.1).

2.9. Data resources

The accession number for the raw and processed data files is available in SRA: SRR9107534.

3. Results

3.1. The generation of Akap4-knockout mice

CRISPR-cas9-edited mice fertilized eggs generated 13 F0 founders, among 32 pups. F1 mice were obtained after the selected F0 mice mated with wild type mice. Female homozygous *Akap4*-KO mice were fertile, but male hemizygous *Akap4*-KO mice were completely sterile despite showing normal mating behavior with successful ejaculation and vaginal plug formation. A frameshift mutation was generated by deleting exon 5 and exon 6 of *Akap4* (Fig. 1A). The predicted length of truncated protein Akap4 is 92 aa, only ~10% of the original protein, so there may well be a nonsense mediated mRNA decay (NMD) incurred which causes the frameshift transcript degradation. Western blotting confirmed the absence of the Akap4 protein in the testis of KO mice (Fig. 1B).

3.2. The assessment of sperm and testis of Akap4-knockout mice

Sperm from the infertile *Akap4*-knockout mice were extracted and analyzed by a CASA system to observe the cytomorphology and motility. As Table 1 shows, the sperm concentration of the KO mice was significantly less than the WT mice. And the viability of sperm from KO mice was also decreased sharply. Moreover, the absence of *Akap4* significantly weakened the motility of sperm which could directly influenced the fertilization (Table 1). Meanwhile, the curvilinear velocity (VCL), straight-line velocity (VSL), average path velocity (VAP), straightness (STR), linearity (LIN) and wobbling (WOB) were all decreased after the *Akap4* loss (Table 1). To make a further investigation, we observed the cytomorphology of sperm from the KO mice and found that the flagella of sperm from the KO mice were severely dysmorphic and the sperm were totally inactive (Fig. 1C). These observations indicate that Akap4 is indispensable for the cytomorphology and motility of sperm.

Papanicolaou staining confirmed the abnormal structure of the sperm from the mutant mice, showing the scattered and curved flagella

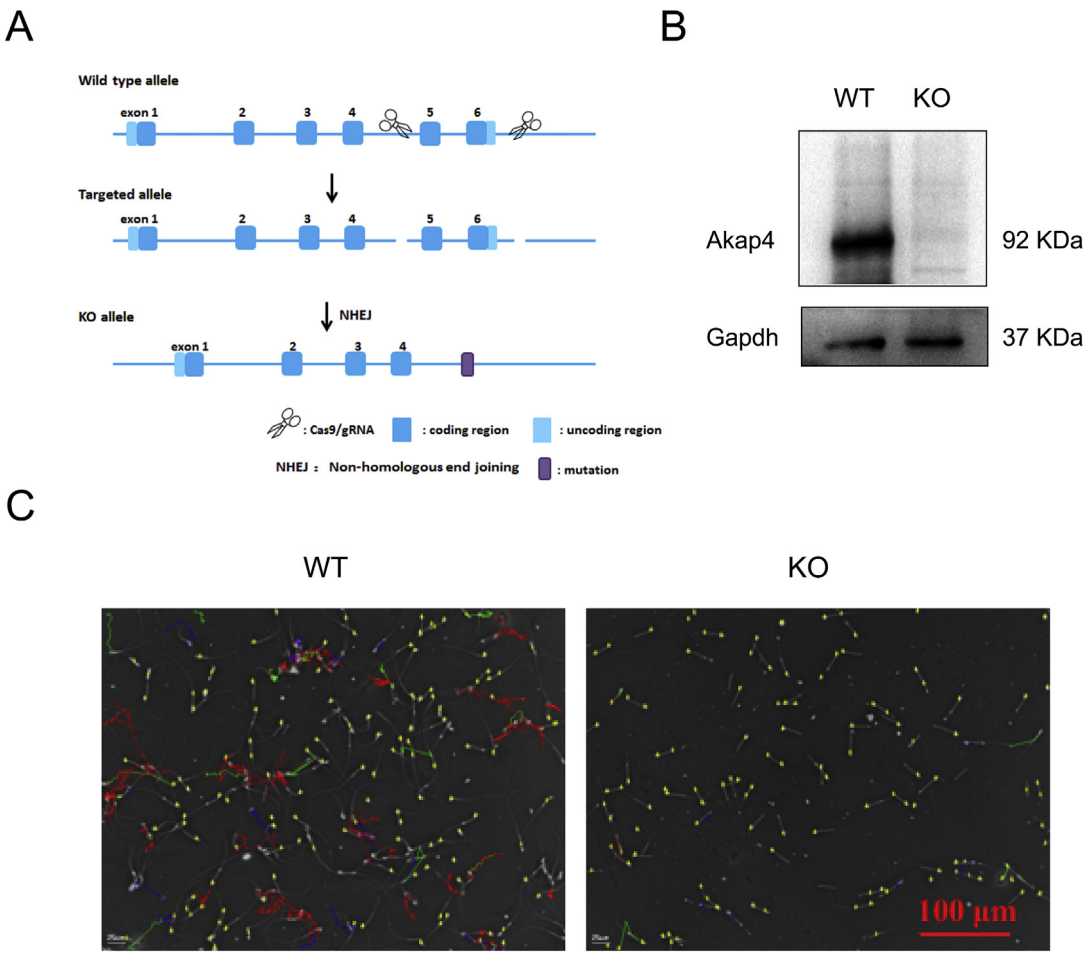

Fig. 1. Deficiency of Akap4 leads to MMAF in mice. (A) The schematic illustration of the targeting strategy for generating KO mice. A frameshift mutation was generated by deleting exon 5 and exon 6 of *Akap4*. (B) Akap4 protein levels in the testis of WT and KO mice. (C) The motility and cytomorphology of sperm from the KO mice. Sperm were analyzed by the Sperm Cytomorphology Analyzer with phase microscopy (Microptic S.L., Spain). The numbers of WT and KO mice were both 7. Red curve represents the path of A-level motility sperm; green curve represents B-level motility sperm; blue curve represents C-level motility sperm; yellow curve represents D-level motility sperm.

(Fig. 2A). To get a deeper observation, we analyzed the structural change of sperm from KO mice by electron microscope. Transmission electron microscope showed that the structure of the fibrous sheath in sperm lacking Akap4 was absent (Fig. 2B). And as the scanning electron microscope demonstrated, the principal piece of flagella lacking Akap4 was reduced in diameter and the tip was curled or splayed apart into finer filaments compared with sperm of WT mice (Fig. 2C). The immunofluorescence staining of Akap4 expression also confirmed the absence of Akap4 protein expression on KO spermatozoa (Fig. 2D).

Since the structure of cauda epididymal sperm were abnormal, we checked into seminiferous tubules and sperm in the testis. HE and PAS staining of testis tissues from WT and the KO mice showed no significant morphological abnormalities (Fig. 3A and B). Transmission electron microscopy (TEM) was applied to examine the structure of the sperm in the testis of KO mice. Our results showed that the absence of fibrous sheath also happened on the sperm in the testis, and no other obvious structural difference was observed in the testis (Fig. 3C and D).

3.3. The single-cell RNA sequencing and analysis of testes of Akap4-knockout mice

The testes of a 26-week WT mouse and a 26-week KO mouse were processed and analyzed in a pipeline of 10XGenomic single-cell RNA sequencing. The WT and KO samples had 3659 and 3145 cells identified, respectively. The general comparison of WT and KO cells gave rise to three significantly changed genes, namely, *Akap4*, *Haspin*, and *Ccdc38*. All three genes were decreased in expression of the KO mouse compared with the WT one. Interestingly, both *Haspin* (Histone H3 Associated

Table 1
CASA analysis of sperm from *Akap4*-knockout mice.

Parameter	WT	*KO*	P-value
Concentration (mill/ml)	49.3 ± 8.7	34.5 ± 7.3	0.005
Viability (%)	56.1 ± 9.4	11.9 ± 5.4	0.000
Motility (%)			
A-level motility (%)	10.3 ± 1.5	0.4 ± 0.2	0.000
B-level motility (%)	24.6 ± 5.6	2.0 ± 0.9	0.000
C-level motility (%)	21.2 ± 4.4	9.6 ± 4.7	0.000
D-level motility (%)	43.9 ± 9.4	88.1 ± 5.4	0.000
VCL (μm/s)	125.8 ± 7.5	71.0 ± 7.8	0.000
VSL (μm/s)	40.2 ± 1.9	16.0 ± 2.8	0.000
VAP (μm/s)	60.0 ± 3.5	27.1 ± 2.8	0.000
LIN (%)	30.5 ± 3.0	22.1 ± 4.3	0.001
STR (%)	66.6 ± 2.4	57.5 ± 4.8	0.001
WOB (%)	45.8 ± 3.4	38.2 ± 4.8	0.005

A-level motility sperm: the sperm move forward rapidly.
B-level motility sperm: the sperm move forward slowly.
C-level motility sperm: the sperm move non-forward.
D-level motility sperm: the sperm move extremely slowly or keep static.
VCL: curvilinear velocity; VSL: straight-line velocity; VAP: average path velocity.
LIN: linearity; STR: straightness; WOB: wobbling.

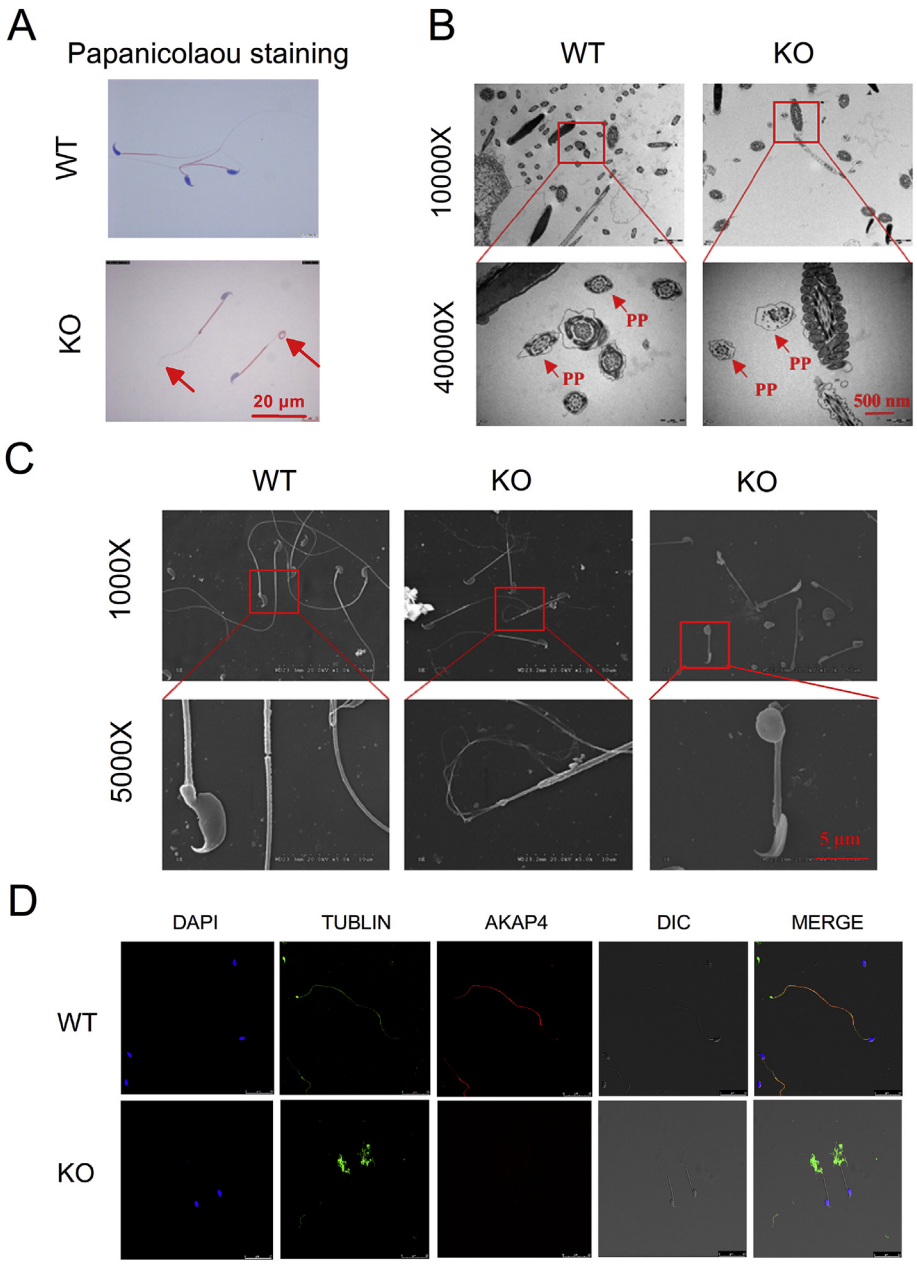

Fig. 2. Abnormal flagella of cauda epididymal sperm from KO mice. (A) Cauda epididymal sperm were gently isolated from WT and KO mice and then observed by Papanicolaou staining. (B) Transmission electron micrographs showing incomplete development of the fibrous sheath of sperm from KO mice. (C) Cauda epididymal sperm isolated from WT and KO mice were observed with scanning electron microscopy (1000X and 5000X magnification, scale bar represents 5 μm). Cauda epididymides from WT and KO mice were fixed and sectioned for the transmission electron microscopy (10000X and 40000X magnification, scale bar represents 500 nm). PP: principal piece. (D) Immunofluorescence staining of Akap4 and Tublin expression in WT and Akap4 KO spermatozoa. Akap4 staining (red) was absent on Akap4 KO spermatozoa (blue, DAPI; scale bars, 25 μm).

Protein Kinase) and *Ccdc38* (Coiled-Coil Domain Containing 38) are involved in normal progression through cell cycle in mitosis, and this indicates that the deficiency of *Akap4* causes not only dysfunctional sperm flagellum, but also incurs cell cycle arrest in the early stage cells of spermatogenesis including spermatogonia, spermatocyte and round spermatid, thus eventually cause the decreased yield of mature sperm.

The t-SNE presentation of testis cells by their single-cell RNA expression showed that testis cells, either in WT or KO, had generally six different cell clusters according to their specific expressional profiles (Fig. 4A). A simple review of KO and WT mice single-cell RNA profiling plots found the major difference occurred in the Elongating spermatids, which was not surprising since *Akap4* gene was supposed to play roles in the terminal stage of spermatogenesis when the round spermatid elongates and taper off at one end to form the mature sperm. Green et al. has validated that *Akap4* was the marker gene of Elongating spermatids (Green et al., 2018), which justifies the major difference between KO and WT shown in Fig. 4A. Interestingly, when the Elongating spermatid cluster zoomed in and was subdivided into four subcategories, there were an obvious increase in type 3 cells and a decrease in type 1 cells, in the KO Elongating spermatids compared with their counterparts in the WT ones (Fig. 4B). The differential expressed genes of type 3 include *St6galnac2* (ST6 N-Acetylgalactosaminide Alpha-2,6-Sialyltransferase 2), *Vasp* (Vasodilator Stimulated Phosphoprotein), and *Nrd1* (Nardilysin Convertase), which are likely involved in cell migration and adhesion (Table S1). The differential expressed genes of type 1 include *Smcp* (Sperm Mitochondria Associated Cysteine Rich Protein), *Car2* (Carbonic Anhydrase 2), and *Oaz3* (Ornithine Decarboxylase Antizyme 3), which are located inside mitochondria (Table S2), while in sperm flagellum, the mitochondria gather in the mitochondrial sheath which forms the middle piece of sperm flagellum.

As afore-mentioned, there were three genes showing general expression changes between WT and KO mice testis, namely, *Akap4*, *Haspin*, and *Ccdc38*. The t-SNE expressional profiling plots confirm the decrease of the three genes, while in different cell clusters, namely,

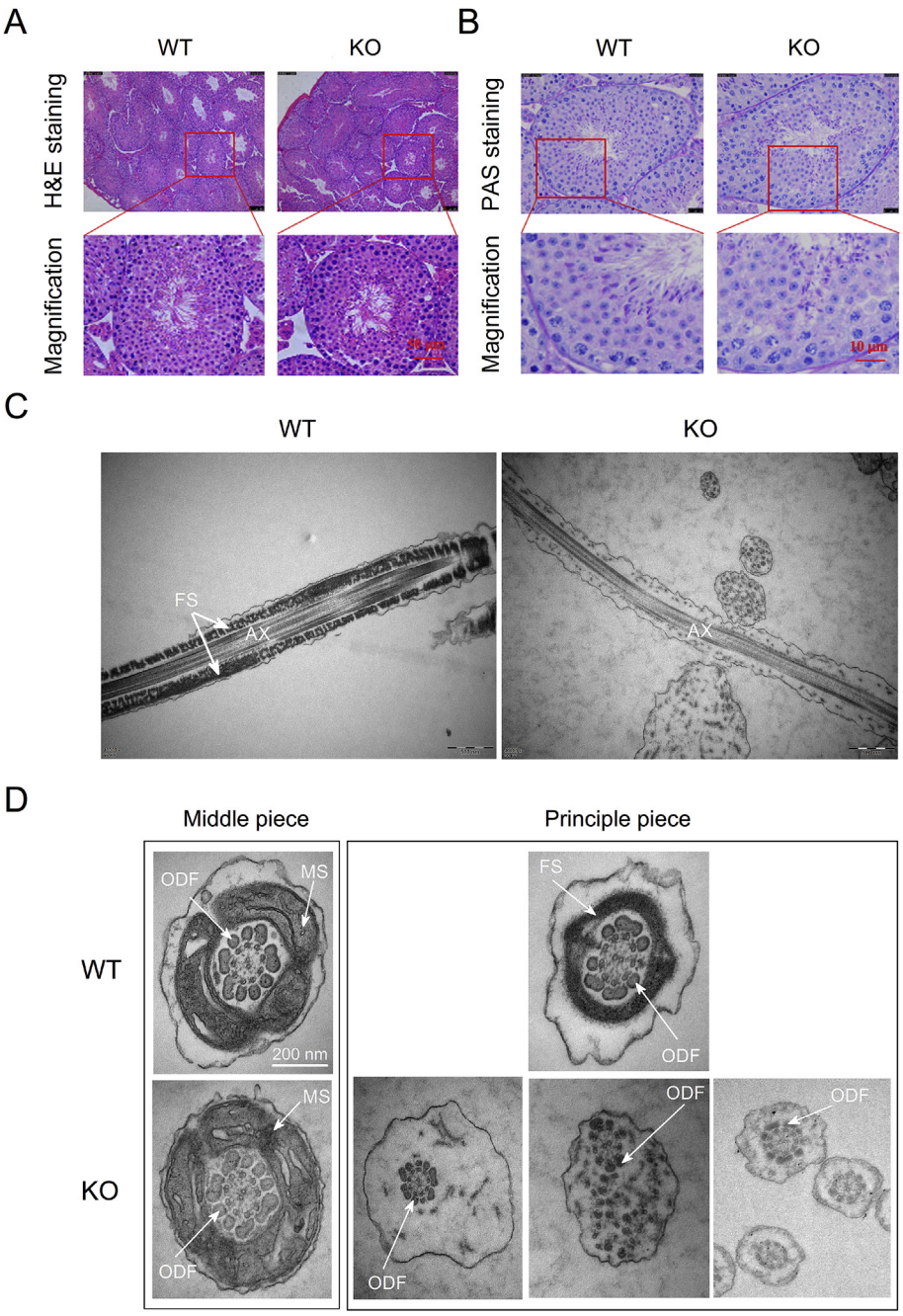

Fig. 3. Structure of testis in *Akap4*-knockout mice. HE staining (A) and PAS staining (B) of testes from WT and the KO mice show no significant morphological abnormalities. (C) Longitudinal view and (D) cross section of a principal piece. Transmission electron micrographs show incomplete development of the fibrous sheath of sperm in different phases of KO mice. The KO TEM image showed the absence of fibrous sheath as well as the abnormal tail coiling and the tail splitting. Testicular tissues from WT and KO mice were fixed and sectioned for the transmission electron microscopy (4000X, 10000X and 40000X magnification, scale bar represents 500 nm). PP: principal piece; R: rib of the fibrous sheath; LC: longitudinal column of the fibrous sheath; ODF: outer dense fibers.

Akap4 in Elongating spermatids, *Haspin* in Spermatocytes and Round spermatids, *Ccdc38* in Spermatogonia and Spermatocytes (Fig. 4C). This observation is not counterintuitive, if considering the step-wise differentiation of male gametes in the seminiferous tubules.

In addition, we identified an Unknown cluster in our single cell data, which is located in the vicinity of the Round spermatid cluster (Fig. 4A). The top 5 marker genes of the Unknown cluster are *1700025N23Rik, Hdac11, Pnmal2, Gm29825* and *Malat1*. Their expression patterns are shown in Fig. 5. *1700025N23Rik, Hdac11, Pnmal2* and *Gm29825* are exclusively highly expressed in the Unknown cluster; *1700025N23Rik, Hdac11, Gm29825* and *Malat1* have not been identified as marker genes for any known cell types, except *Pnmal2*. *1700025N23Rik*, *Pnmal2* and *Gm29825* are novel genes; the roles of the 5 marker genes in spermatogenesis remain undiscovered.

3.4. The proteomic analysis of testes of Akap4-knockout mice

Two paired proteomic studies were conducted, one study including two 21-week KO mice (treatment_1 and treatment_2) and one 18-week WT mouse (control_1), another study including one 27-week KO mouse (treatment_3) and one 28-week WT mouse (control_2). Close to half of mice genome proteins were found to be expressed in the testes, and the significantly fold-changed proteins by the comparisons among three treatments and two controls were listed in Table 2.

There were two proteins significantly decreased in their abundances when comparing the KO mice and the WT ones, namely, Akap4 per se, and its prototype Akap82. Although there were other proteins increased or decreased significantly in one or two paired comparisons, it looked like that the dramatic and common change happened only in Akap4 and

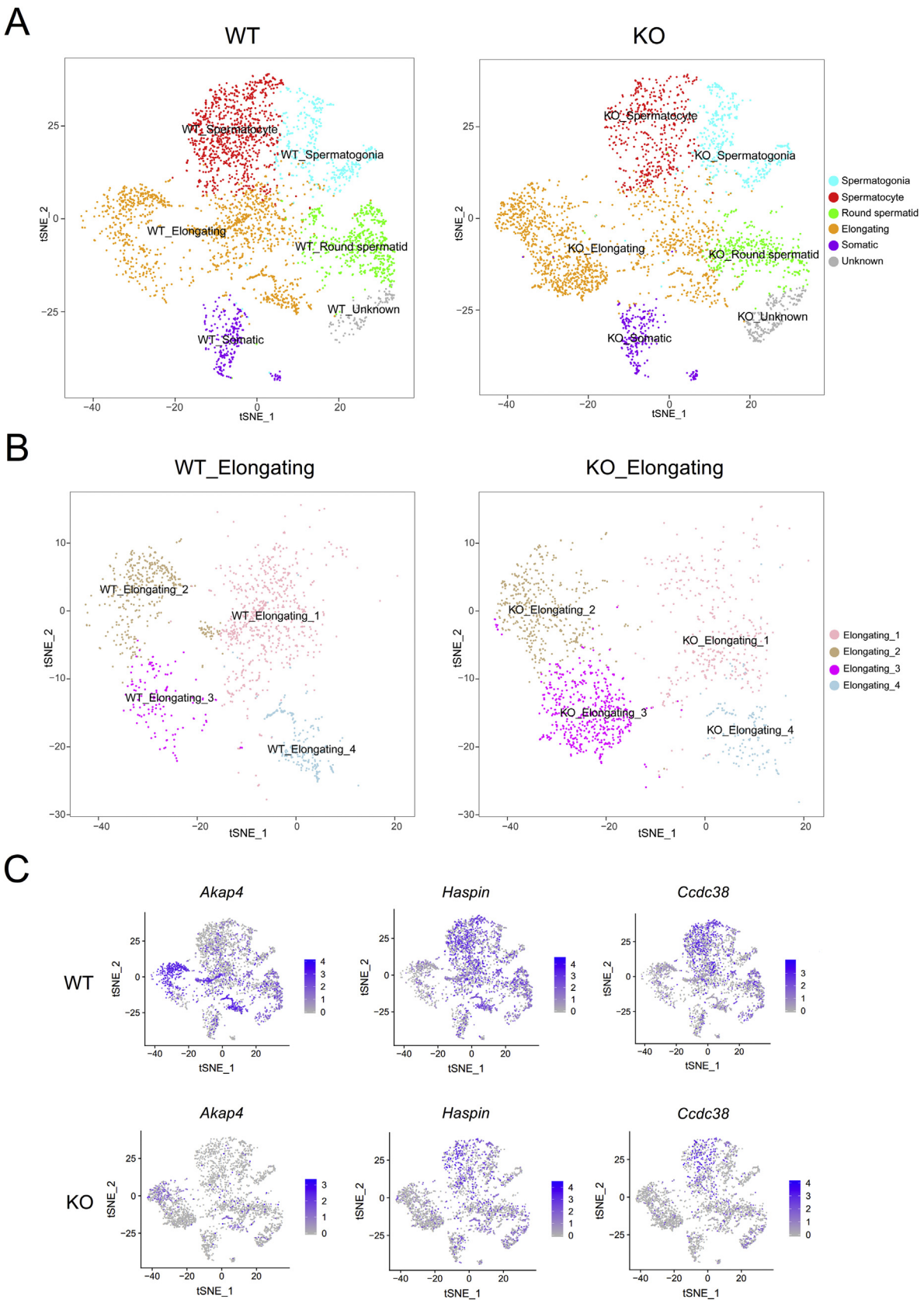

Fig. 4. (A) t-SNE plot showed the expression of testis cells. Different colors stand for specific cell clusters, including Spermatocyte (red), Elongating spermatid (orange), Round spermatid (green), Spermatogonia (cyan), Somatic cell (purple), and Unknown cell (grey). The major difference between WT and KO exists in the cluster of Elongating spermatid. (B) t-SNE presentation of the Elongating spermatid cluster. Different colors stand for specific sub-clusters. When comparing WT and KO, it is obvious that the type 3 cells increase and the type 1 cells decrease in KO elongating cells. (c) t-SNE presentation of three differential expressed genes, indicating their distribution in different clusters and relative expression magnitude.

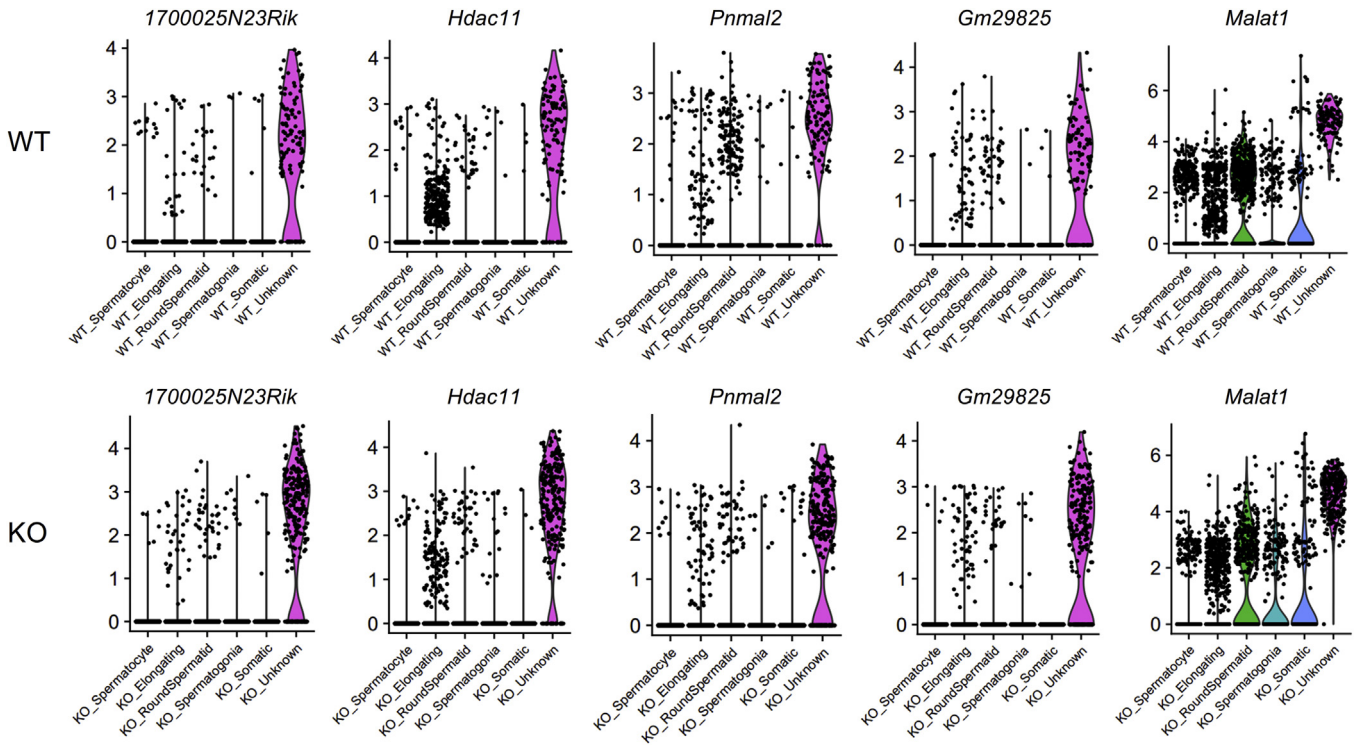

Fig. 5. Violin plot showed the expression patterns of the top 5 marker genes for the Unknown clusters of WT and KO.

Table 2
Number of proteins identified in 3 proteomic studies.

Compared samples	Number of proteins identified	Number of proteins significantly changed	Number of proteins significantly up-regulated	Number of proteins significantly down-regulated
Treatment_1 vs. control_1	8753	55	43	12
Treatment_2 vs. control_1	8754	26	16	10
Treantment_3 vs. control_2	7194	39	14	25
Overlap	7193	2	0	2

its precedent form.

4. Discussion

As a unique cytoskeletal structure, the fibrous sheath is suggested to serve as a scaffold for proteins in signaling pathways involved in sperm maturation, motility, capacitation, and glycolysis (Eddy et al., 2003). Akap4 is the first AKAP to be described as associated with the sperm flagellum and is also the most abundant protein in the sperm fibrous sheath (Miki et al., 2002; Eddy et al., 2003). The physiological role of fibrous sheath and its associated proteins has not been clearly determined. We utilized the genetic technology of the CRISPR-Cas9 system and generate an *Akap4*-knockout mouse line.

Male *Akap4*−/− were infertile, with reduced sperm number and viability. Testicular sections suggested spermiogenesis is normal. The structure of the fibrous sheath was absent, but the other structure of cytoskeletal components of the flagellum were complete in morphology. *Akap4*-knockout mice created by CRE/loxP method have been reported (Miki et al., 2002). Consistent with their results, sperm from KO mice failed to show progressive motility and male mice were infertile. The definitive fibrous sheath did not develop, and proteins usually associated with the fibrous sheath were absent or substantially reduced in amount. However, obvious differences were still found between the two researches. Firstly, in their report, the number of epididymal sperm from mutant mice was higher but not significantly different from those of wild type males. In contrast, epididymal sperm concentration in our KO mice was significantly lower compared with those of WT males. According to the component of the spermatids the seminiferous tubules could be divided into 12 stages (I-XII) (Hess and Renato de Franca, 2008). Testicular sections showed that no obvious defects are found at any stage of spermiogenesis, and all of the components in the WT testis could be found in the KO testis. Considering the sharply decreased viability and motility of sperm from KO mice, it is possible that fewer sperm swam out from the minced cauda epididymis. However, we still could not exclude the possibility that less sperm are generated in *Akap4*-knockout mice. Furthermore, the relative length of the principle piece of sperm from mutant mice averaged about half that of sperm from wild type mice in their results, and they suggest that Akap4 has a role in flagellar elongation and/or in determining or maintaining flagellar length (Miki et al., 2002). We did not find obvious difference in the length of flagellum between the two types of mice under Papanicolaou staining and scanning electron microscopy. Miki et al. measured the principle piece under phase microscopy and they also mentioned it was not easy to measure clearly because the tail was curled or was obscured. We did find the tail of the sperm was scattered into pieces or curved into a sphere. Both of the two shapes would create an illusion that the length of the sperm is shortened. Consequently, we consider Akap4 does not have a role in flagellar elongation and/or in determining or maintaining flagellar length. The different phenotypes between our mutant mice and that reported by Miki et al. (2002) likely result from the disruption of different regions of the *Akap4* gene. This kind of phenomenon is not uncommon in mouse mutagenesis studies (Weissmann and Aguzzi, 1999; Wang et al., 2007). This could be explained by the different truncated proteins that were expressed after genomic modification, although they might be expressed at very low levels.

The proteomic and single-cell RNA analysis of KO testes are unprecedented, as we are aware. In proteomic study, we found Akap4 protein was the only significantly changed protein in the repeated tests, and this

meant *Akap4* gene is probably a downstream gene of spermatogenesis, so it plays more a structural role than an upstream modulator which influences a bunch of downstream genes. On the other hand, single-cell RNA sequencing of testes revealed in-depth details of testis cell spectrum and the pathological alteration in KO mice. We successfully categorized the testes cells into six types, i.e., Spermatogonia, Spermatocytes, Round spermatids, Elongating spermatids, Somatic cells, and Unknown cells (Table S3). We noticed that the significantly changed three genes in the total cell population, namely, *Akap4*, *Haspin*, and *Ccdc38*. *Ccdc38* (Coiled-Coil Domain Containing 38) is a testes-specific gene, mainly localized in the nuclei of spermatogonia and spermatocytes of the seminiferous tubules (Green et al., 2018; Lin et al., 2016). Lin et al. reported that Ccdc38 interacted with ubiquitinated histone H2A in mouse testis, indicating its important role in mouse spermatogenesis (Lin et al., 2016). *Haspin* (Histone H3 Associated Protein Kinase), which is expressed at high level in testis of mammals (Tanaka et al., 1999) (particularly in round spermatids) is required for mitotic histone H3 Thr 3 phosphorylation and normal metaphase chromosome alignment (Dai et al., 2005). RNAi experiments suggested that depletion of *Haspin* incur premature loss of cohesin binding and sister chromatid association in mitosis, resulting in activation of the spindle assembly checkpoint and mitotic arrest (Dai et al., 2006). On the other hand, *Akap4* (A kinase anchor protein 4), which is expressed in the cytoplasm of round and elongated spermatids (Hu et al., 2009) was recognized as the marker of elongating spermatids (Green et al., 2018). AKAP4 has two binding sites for PKA (Miki and Eddy, 1999); AKAP4 is also an ERK1/2 substrate in human spermatozoa (Rahamim Ben-Navi et al., 2016). In summary, both *Ccdc38* and *Haspin* are involved in histone modification; *Ccdc38* is enriched in spermatogonia and spermatocytes, while *Haspin* and *Akap4* is enriched in round spermatid and spermatozoa, respectively. We thus speculate a sequential feedback from spermatozoa to spermatid, then to spermatocytes and spermatogonia. We admit that this hypothesis is primitive and needs to be verified in a more systematic way in future.

We also observed an obvious but expected expression pattern alteration of elongating cells when comparing WT with KO, which was justified by the finding that *Akap4* was the marker gene of Elongating cells (Green et al., 2018). The zoom-in study on the elongating cells showed in the KO testis an increase of cells with differential expressed genes involved in cell adhesion and migration (Table S1), while a decrease of cells marked by genes located in mitochondrial sheath (Table S2). These observations provide a piece of circumstantial evidence that spermatogenesis is a step-wise procedure which is under strict regulation of a sophisticated and fine-tuned gene network, reflected by the sequential development of microscopic structures of sperm and the domino-style differentiation of gametes stem cells.

In addition, we identified an Unknown cluster in our single cell data, which is adjacent to the Round spermatid cluster (Fig. 4A). The top 5 marker genes of the Unknown cluster are *1700025N23Rik, Hdac11, Pnmal2, Gm29825* and *Malat1* (Fig. 5). As a non-coding RNA, 1700025N23Rik is exclusively expressed in testis of adult mouse. *Hdac11* encodes a class IV histone deacetylase, which is highly expressed in testis and cerebellum in adult mouse. *Hdac11* plays an important role in transcriptional regulation, cell cycle progression and developmental events; previous research has validated its essential function in Hodgkin lymphoma (Buglio et al., 2011) and neutrophil biology (Sahakian et al., 2017). *Pnmal2* (PNMA-like 2) is a novel coding gene; *Gm29825* is predicted to be a coding gene exclusively expressed in testis of adult mouse. The product of *Malat1* may act as a transcriptional regulator for numerous genes, including some genes involved in cancer metastasis and cell migration. Gutschner et al. proved that the *MALAT1*-deficient cells are impaired in migration and form fewer tumor nodules in a mouse xenograft, implying Malat1 as a biomarker for lung cancer metastasis (Gutschner et al., 2013). However, the roles of the 5 genes in spermatogenesis remain undiscovered. Moreover, it is worthwhile to mention that the Unknown cluster is distinct from the "Unknown" cell type recognized by Green et al. since 4 of the top 5 marker genes (*1700025N23Rik, Hdac11, Gm29825* and *Malat1*) have not been classified into any known cell types. This implies that a novel cell type may exist in testis of mouse and further investigation on the novel marker genes may provide insights in germ cell development and in vivo gametogenesis.

Acknowledgements

This work was supported by the National Natural Science Foundation of China 81701451 (N. L.), the National Key Research and Development Program of China SQ2018YFC100269-03 (W. X.) and the Natural Science Foundation of Guangdong Province of China 2018A030313538 (X. F.).

Appendix A. Supplementary data

Supplementary data to this article can be found online at https://doi.org/10.1016/j.ydbio.2019.06.017.

References

Baccetti, B., Collodel, G., Estenoz, M., Manca, D., Moretti, E., Piomboni, P., 2005. Gene deletions in an infertile man with sperm fibrous sheath dysplasia. Hum. Reprod. 20, 2790–2794.
Bolger, A.M., Lohse, M., Usadel, B., 2014. Trimmomatic: a flexible trimmer for Illumina sequence data. Bioinformatics 30, 2114–2120.
Buglio, D., Khaskhely, N.M., Voo, K.S., Martinez-Valdez, H., Liu, Y.J., Younes, A., 2011. HDAC11 plays an essential role in regulating OX40 ligand expression in Hodgkin lymphoma. Blood 117, 2910–2917.
Carrera, A., Gerton, G.L., Moss, S.B., 1994. The major fibrous sheath polypeptide of mouse sperm: structural and functional similarities to the A-kinase anchoring proteins. Dev. Biol. 165, 272–284.
Dai, J., Sultan, S., Taylor, S.S., Higgins, J.M., 2005. The kinase haspin is required for mitotic histone H3 Thr 3 phosphorylation and normal metaphase chromosome alignment. Genes Dev. 19, 472–488.
Dai, J., Sullivan, B.A., Higgins, J.M., 2006. Regulation of mitotic chromosome cohesion by haspin and aurora B. Dev. Cell 11, 741–750.
Eddy, E.M., Toshimori, K., O'Brien, D.A., 2003. Fibrous sheath of mammalian spermatozoa. Microsc. Res. Tech. 61, 103–115.
Fawcett, D.W., 1975. The mammalian spermatozoon. Dev. Biol. 44, 394–436.
Green, C.D., Ma, Q., Manske, G.L., Shami, A.N., Zheng, X., Marini, S., Moritz, L., Sultan, C., Gurczynski, S.J., Moore, B.B., et al., 2018. A comprehensive roadmap of murine spermatogenesis defined by single-cell RNA-seq. Dev. Cell 46, 651–667 e610.
Gutschner, T., Hammerle, M., Eissmann, M., Hsu, J., Kim, Y., Hung, G., Revenko, A., Arun, G., Stentrup, M., Gross, M., et al., 2013. The noncoding RNA MALAT1 is a critical regulator of the metastasis phenotype of lung cancer cells. Cancer Res. 73, 1180–1189.
Hamada, A., Esteves, S.C., Nizza, M., Agarwal, A., 2012. Unexplained male infertility: diagnosis and management. Int. Braz J. Urol. 38, 576–594.
Hess, R.A., Renato de Franca, L., 2008. Spermatogenesis and cycle of the seminiferous epithelium. Adv. Exp. Med. Biol. 636, 1–15.
Hu, Y., Yu, H., Pask, A.J., O'Brien, D.A., Shaw, G., Renfree, M.B., 2009. A-kinase anchoring protein 4 has a conserved role in mammalian spermatogenesis. Reproduction 137, 645–653.
Kumar, V., Jagadish, N., Suri, A., 2017. Role of A-Kinase anchor protein (AKAP4) in growth and survival of ovarian cancer cells. Oncotarget 8, 53124–53136.
La Salle, S., Sun, F., Handel, M.A., 2009. Isolation and short-term culture of mouse spermatocytes for analysis of meiosis. Methods Mol. Biol. 558, 279–297.
Lin, S.R., Li, Y.C., Luo, M.L., Guo, H., Wang, T.T., Chen, J.B., Ma, Q., Gu, Y.L., Jiang, Z.M., Gui, Y.T., 2016. Identification and characteristics of the testes-specific gene, Ccdc38, in mice. Mol. Med. Rep. 14, 1290–1296.
Miki, K., Eddy, E.M., 1999. Single amino acids determine specificity of binding of protein kinase A regulatory subunits by protein kinase A anchoring proteins. J. Biol. Chem. 274, 29057–29062.
Miki, K., Willis, W.D., Brown, P.R., Goulding, E.H., Fulcher, K.D., Eddy, E.M., 2002. Targeted disruption of the Akap4 gene causes defects in sperm flagellum and motility. Dev. Biol. 248, 331–342.
Rahamim Ben-Navi, L., Almog, T., Yao, Z., Seger, R., Naor, Z., 2016. A-Kinase Anchoring Protein 4 (AKAP4) is an ERK1/2 substrate and a switch molecule between cAMP/PKA and PKC/ERK1/2 in human spermatozoa. Sci. Rep. 6, 37922.
Sahakian, E., Chen, J., Powers, J.J., Chen, X., Maharaj, K., Deng, S.L., Achille, A.N., Lienlaf, M., Wang, H.W., Cheng, F., et al., 2017. Essential role for histone deacetylase 11 (HDAC11) in neutrophil biology. J. Leukoc. Biol. 102, 475–486.
Satija, R., Farrell, J.A., Gennert, D., Schier, A.F., Regev, A., 2015. Spatial reconstruction of single-cell gene expression data. Nat. Biotechnol. 33, 495–502.
Shen, B., Zhang, J., Wu, H., Wang, J., Ma, K., Li, Z., Zhang, X., Zhang, P., Huang, X., 2013. Generation of gene-modified mice via Cas9/RNA-mediated gene targeting. Cell Res. 23, 720–723.
Shen, Y., Zhang, F., Li, F., Jiang, X., Yang, Y., Li, X., Li, W., Wang, X., Cheng, J., Liu, M., et al., 2019. Loss-of-function mutations in QRICH2 cause male infertility with multiple morphological abnormalities of the sperm flagella. Nat. Commun. 10, 433.

Tanaka, H., Yoshimura, Y., Nozaki, M., Yomogida, K., Tsuchida, J., Tosaka, Y., Habu, T., Nakanishi, T., Okada, M., Nojima, H., et al., 1999. Identification and characterization of a haploid germ cell-specific nuclear protein kinase (Haspin) in spermatid nuclei and its effects on somatic cells. J. Biol. Chem. 274, 17049–17057.

Turner, R.M., 2003. Tales from the tail: what do we really know about sperm motility? J. Androl. 24, 790–803.

Wang, Y., Zhang, H.X., Sun, Y.P., Liu, Z.X., Liu, X.S., Wang, L., Lu, S.Y., Kong, H., Liu, Q.L., Li, X.H., et al., 2007. Rig-I-/- mice develop colitis associated with downregulation of G alpha i2. Cell Res. 17, 858–868.

Weissmann, C., Aguzzi, A., 1999. Perspectives: neurobiology. PrP's double causes trouble. Science 286, 914–915.

Young, S.A., Miyata, H., Satouh, Y., Aitken, R.J., Baker, M.A., Ikawa, M., 2016. CABYR is essential for fibrous sheath integrity and progressive motility in mouse spermatozoa. J. Cell Sci. 129, 4379–4387.